JOURNAL OF VIROLOGY, Nov. 2010, p. 11440–11447 Vol. 84, No. 21
0022-538X/10/$12.00 doi:10.1128/JVI.01030-10

Cytotoxicity of ORF3 Proteins from a Nonpathogenic and a Pathogenic Porcine Circovirus▽

Mark Chaiyakul,[1,2] Karolynn Hsu,[1] Rkia Dardari,[1] Frank Marshall,[1,3] and Markus Czub[1,2]*

Department of Production Animal Health, Faculty of Veterinary Medicine,[1] and Department of Microbiology and Infectious Diseases, Faculty of Medicine,[2] University of Calgary, Calgary, Alberta, Canada, and Marshall Swine Health Services, Camrose, Alberta, Canada[3]

Received 12 May 2010/Accepted 21 August 2010

Porcine circovirus type 2 (PCV2) infection is associated with significant and serious swine diseases worldwide, while PCV1 appears to be a nonpathogenic virus. Previous studies demonstrated that the ORF3 protein of PCV2 (PCV2ORF3) was involved in PCV2 pathogenesis via its proapoptotic capability (J. Liu, I. Chen, Q. Du, H. Chua, and J. Kwang, J. Virol. 80:5065-5073, 2006). If PCV2ORF3-induced apoptosis is a determinant of virulence, PCV1ORF3 is hypothesized to lack this ability. The properties of PCV1 and PCV2 ORF3, expressed as fusion proteins to an enhanced green fluorescent protein (eGFP), were characterized with regard to their ability to cause cellular morphological changes, detachment, death, and apoptosis. PCV1ORF3 significantly induced more apoptotic cell death and was toxic to more different cell types than PCV2ORF3 was. PCV1ORF3-associated cell death was caspase dependent. PCV1ORF3 also induced poly(ADP-ribose) polymerase 1 (PARP) cleavage; however, whether PARP was involved in cell death requires further studies. Truncation of PCV1 and elongation of PCV2 ORF3 proteins revealed that the first 104 amino acids contain a domain capable of inducing cell death, whereas the C terminus of PCV1ORF3 contains a domain possibly responsible for enhancing cell death. These results suggest that the pathogenicity of PCV2 for pigs is either not determined or not solely determined by the ORF3 protein.

Lymphocyte depletion and the presence of porcine circovirus type 2 (PCV2) genome and antigens (4, 6, 21) are hallmarks of PCV-associated disease (PCVAD), a wasting and immunosuppressive ailment of postweaned pigs. Despite two decades of research, little is known about the molecular pathogenesis of PCVAD.

PCV2 is the smallest known autonomous vertebrate virus containing a 1.7-kb single-stranded, ambisense DNA genome (32). The virus has two major open reading frames (ORFs) that encode the replication proteins (Rep and Rep′) involved in the initiation of virus replication (17) and a capsid protein (Cap), forming the capsid of the virion (32). A third ORF encodes an ORF3 protein that has been characterized as an inducer of apoptosis (14). Abrogation of ORF3 expression attenuated PCV2 pathogenesis in BALB/c mice (13) and specific-pathogen-free piglets (9). This led to the hypothesis that ORF3 is involved in PCV2 pathogenesis by inducing apoptosis in infected lymphocytes, leading to lymphocyte depletion and ultimately immunosuppression (13, 25). The closely related, yet nonpathogenic porcine circovirus type 1 (PCV1) also has a third open reading frame, but the properties of the ORF3 protein of PCV1 (PCV1ORF3) have not been characterized. Analysis of over 250 PCV2 variants and 30 PCV1 variants shows a consistent single-nucleotide substitution in the *ORF3* coding sequence of PCV2 (*PCV2ORF3*), resulting in a stop codon and a protein that is half the size of PCV1ORF3 (PCV2ORF3 is made up of 104 amino acids [aa] compared to PCV1ORF3, which is made up of 206 aa). A comparison between PCV1 and PCV2 ORF3 translated regions reveals only 60% amino acid sequence identity (5), making ORF3 the most variable protein among the three identified major proteins of PCV. If ORF3 is a determinant of virulence of PCV2 via its apoptotic capability, PCV1ORF3 is hypothesized to lack the ability to induce apoptotic cell death. This report demonstrates the differences in cytotoxic properties between PCV1ORF3 and PCV2ORF3. Interestingly, PCV1ORF3 appeared to be more cytotoxic than PCV2ORF3, activating a caspase-dependent apoptotic pathway and potentially a caspase-independent, poly(ADP-ribose) polymerase 1 (PARP) cleavage pathway. Further analysis of truncated PCV1ORF3 and elongated PCV2ORF3 showed that different ORF3 proteins had similar patterns of cytotoxicity, although full-length PCV1ORF3 was the most potent inducer of cell death.

MATERIALS AND METHODS

Generation of recombinant eukaryotic expression vectors. Coding sequences of the *ORF3* genes were PCR amplified from synthetic PCV1 and PCV2 genomes (DNA 2.0, Menlo Park, CA) by using primers. For *PCV1ORF3*, primers 5′-ATTCTCGAGCCATGATATCCATCCCACCACT-3′ (forward) (nucleotide positions 658 to 639) and 5′-AATGGATCCTCAGTGAAAATGCCAAGCAAG-3′ (reverse) (nucleotide positions 38 to 58) were used. For *PCV2ORF3*, primers 5′-ATTCTCGAGCCATGGTAACCATCCCACCACTT-3′ (forward) (nucleotide positions 671 to 651) and 5′-AATGGATCCTTACTTATTGAATGTGGAGC-3′ (reverse) (nucleotide positions 357 to 376) were used. PCR was performed with iProof high-fidelity DNA polymerase (Bio-Rad, Mississauga, Ontario, Canada) in a GeneAmp PCR system 9700 (PE Applied Biosystems, Carlsbad, CA). PCR consisted of the following: a predenaturation step (30 s at 98°C); (ii) 36 cycles, where 1 cycle consisted of a denaturation step (10 s at 98°C), an annealing step (30 s at 60°C), and an extension step (60 s at 72°C); and (iii) a final extension step (10 min at 72°C). PCR products of expected size were purified using a QIAquick gel extraction kit (Qiagen, Mississauga, Ontario, Canada). The BamHI/XhoI fragments of *ORF3* were cloned into the correspond-

* Corresponding author. Mailing address: Faculty of Veterinary Medicine, University of Calgary, 3330 Hospital Drive NW, Calgary, Alberta T2N 4N1, Canada. Phone: (403) 220-4744. Fax: (403) 210-7882. E-mail: m.czub@ucalgary.ca.

▽ Published ahead of print on 1 September 2010.

ing sites of the eukaryotic expression plasmid peGFP-C1 (Clontech, Mountain View, CA) generating N-terminal enhanced green fluorescent protein (eGFP) fusion proteins under the control of a human cytomegalovirus promoter.

To generate a truncated PCV1ORF3 (eGFP-PCV1ORF3:Y105*) that resembles the analogous PCV2ORF3, a change of tyrosine residue (Y) to a stop codon (*) at amino acid position 105 was required. To generate an elongated PCV2ORF3 (eGFP-PCV2ORF3:*105Y), a substitution of a stop codon (*) to a tyrosine residue (Y) at amino acid position 105 was achieved through a two-step procedure. *ORF3* genes were first amplified from the viral genomes by using primers. To create truncated PCV1ORF3, primers 5′-ATTCTCGAGCCATGATATCCATCCCACCACT-3′ (forward) (nucleotide positions 658 to 639) and 5′-AATGGATCCTTACTTATCGAGTGTGGAGC-3′ (reverse) (nucleotide positions 344 to 363) were used. To create elongated PCV2ORF3, primers 5′-ATTCTCGAGCCATGGTAACCATCCCACCACTT-3′ (forward) (nucleotide positions 671 to 651) and 5′-AATGGATCCTCACCCAGCAAGAAGAATGG-3′ (reverse) (nucleotide positions 54 to 70) were used. PCR was performed with 1× PCR *Taq* plus master mix (Applied Biological Materials Inc., Richmond, British Columbia, Canada) and consisted of a predenaturation step (10 min at 94°C), followed by 35 cycles, with 1 cycle consisting of denaturation (60 s at 94°C), annealing (60 s at 60°C), and extension at (60 s at 72°C), and a final extension step (10 min at 72°C). The BamHI/XhoI fragments of *ORF3* were cloned into peGFP-C1 in a manner similar to that described previously for the authentic *ORF3* genes. To create an elongated PCV2ORF3, one base mutation was introduced using a QuikChange site-directed mutagenesis kit (Stratagene, La Jolla, CA) with 50 ng of DNA template from the first step and 150 ng of the following mutagenesis primers: 5′-CTGCAGTAAAGAAGGCAACATACTGATTGAGTGTGGAGCTC-3′ (forward) (nucleotide positions 338 to 378) and 5′-GAGCTCCACACTCAATCAGTATGTTGCCTTCTTTACTGCAG-3′ (reverse) (nucleotide positions 378 to 338). PCR was performed with 1× *Taq* DNA polymerase (Fermentas, Burlington, Ontario, Canada) and consisted of a predenaturation step (2 min at 95°C), followed by 12 cycles, with 1 cycle consisting of denaturation (1 min at 95°C), annealing (1 min at 50°C), and extension (6 min at 68°C), and a final extension step at 68°C for 8 min. All *ORF3* sequences were verified by sequencing (Eurofins MWG Operon, Huntsville, AL).

Cells. Human embryonic kidney epithelial 293T and carcinomic human alveolar basal epithelial lung A549 cell lines were maintained in Dulbecco's modified Eagle medium (Sigma-Aldrich, Oakville, Ontario, Canada) with 10% fetal bovine serum, 2% penicillin-streptomycin solution, and 4% 200 mM L-glutamine at 37°C and 5% CO_2. PCV-free porcine kidney epithelial PK-15 cell line and primary pig kidney epithelial cells (PPKCs) were maintained in Eagle's minimum essential medium (Sigma-Aldrich) with 10% fetal bovine serum, 2% penicillin-streptomycin solution, and 4% 200 mM L-glutamine. PPKCs derived from the kidney of a healthy pig free of PCV1 and PCV2 were used starting from passages 4 to 16.

Transfection. The wells of a 12-well plate (3.8 cm^2 per well) were coated with poly-D-lysine (Sigma-Aldrich) and cells were seeded 1 day prior to transfection in growth medium without antibiotics (1 ml per well in a 12-well plate). When the cells were 70 to 80% confluent, 2 μg of DNA was transfected into the cells in each well with Lipofectamine 2000 (Invitrogen, Burlington, Ontario, Canada). One day after transfection, 1 ml of new growth medium without antibiotics was added to each well that was to be analyzed 48 h after transfection.

Western blot analysis. Whole-cell lysates were resolved by 13% sodium dodecyl sulfate-polyacrylamide gel electrophoresis (SDS-PAGE) and blotted onto polyvinylidene fluoride (PVDF) membranes (GE Healthcare, Baie d'Urfe, Quebec, Canada) via a semidry transfer method (Bio-Rad). To prevent nonspecific binding, the membranes were blocked in phosphate-buffered saline containing Tween 20 (PBST) at pH 7.4 (140 mM NaCl, 2.7 mM KCl, 6.5 mM Na_2HPO_4, 1.5 mM KH_2PO_4, 0.1% Tween 20) with 5% skim milk for 1 h at room temperature or overnight at 4°C. They were then incubated with primary antibody for 1 h at room temperature or overnight at 4°C, washed three times with PBST for 5 min each time, incubated with secondary antibody conjugated to horseradish peroxidase for 1 h at room temperature, and washed again three times with PBST before incubation with an enhanced chemiluminescent substrate reagent mix (GE Healthcare) at room temperature for 5 min. Membranes were analyzed with a VersaDoc 5000 MP imaging system (Bio-Rad) and Quantity One software (Bio-Rad). Primary antibodies included mouse anti-GFP (sc-9996; Santa Cruz Biotechnology, Santa Cruz, CA), rabbit anti-PARP (P7605; Sigma-Aldrich), rabbit anti-mitogen-activated protein kinase (anti-MAPK) (M7927; Sigma-Aldrich), and rabbit anti-β-actin (G046; Applied Biological Materials Inc.).

Cell detachment assay. Detached cells were collected from the supernatant and one washing (1 ml) of adherent cells. The pellet of detached cells was resuspended in 50 μl of 1× PBS. After one wash, adherent cells were trypsinized with 200 μl of 0.25% trypsin-EDTA solution (Sigma-Aldrich) and resuspended in 500 μl of growth medium to make a total volume of 700 μl. Detached and adherent cells were counted using a hemocytometer to determine the percentage of detached cells.

Cell viability assay. All cells, including both detached and adherent cells, were collected, centrifuged at 2,000 rpm for 3 min, washed twice with PBS, and resuspended in PBS at 1×10^6 cells/ml. For each treatment, 100 μl of cell suspension was stained with 5 μl of propidium iodide (PI) (BD Biosciences, Mississauga, Ontario, Canada) for 5 to 10 min at room temperature. Four hundred microliters of PBS was added to each tube prior to fluorescence-activated cell sorting (FACS) analysis.

Phosphatidylserine (PS) externalization detection assay. All cells were collected by centrifugation, washed twice with PBS, and resuspended in annexin V-binding buffer at 1×10^6 cells/ml. Each sample was stained with 1 μl of 7-amino-actinomycin D (7-AAD) (Sigma-Aldrich) and 5 μl of annexin V-phycoerythrin (AV-PE) (BD Biosciences) for 15 min at room temperature in the dark. Subsequently, 400 μl of 1× annexin V-binding buffer was added to each tube prior to FACS analysis. Etoposide (Sigma-Aldrich), an apoptosis-inducing chemical, was used as a positive control in this assay.

Cell cycle analysis. All cells were collected by centrifugation, washed twice with PBS, and fixed in ice-cold 70% ethanol for at least 1 h at 4°C. Fixed cells were washed twice with PBS, resuspended in 100 μl of 50-μg/ml PI solution (Invitrogen) containing 5 μl of 10 μg/ml RNase A (Invitrogen) working solution that had been boiled for 5 min, and incubated at 37°C for 45 min prior to FACS analysis.

PARP cleavage detection assay. Whole-cell lysates were subjected to Western blot analysis, using rabbit anti-PARP antibody (Sigma-Aldrich).

Pancaspase inhibitor assay. At the time of transfection, cells were incubated with a pancaspase inhibitor, benzyloxycarbonyl-L-aspart-1-yl-[(2,6-dichlorobenzoyl)oxy]methane (Z-Asp-CH_2-DCB; Santa Cruz Biotechnology), to different final concentrations not exceeding 100 μM. Cell death (PI staining), apoptosis (AV-PE/7-AAD staining), cell cycle (PI staining), and PARP cleavage were assessed.

Statistical analysis. All statistical analyses were performed using MINITAB software (Minitab Inc., State College, PA). One-way analysis of variance (ANOVA) and Tukey's multiple-comparison tests were performed when assumptions of normality and equal variance were met; otherwise, a nonparametric, Kruskal-Wallis pairwise multiple-comparison (Dunn's) test was conducted. A P value of <0.05 was considered significant. At least two independent trials were conducted for each experiment.

Nucleotide sequence accession numbers. *ORF3* coding regions from PCV1 (GenBank accession number AY184287) and PCV2 (GenBank accession numbers EF394779, AY094619, and AY847748) were used in this study.

RESULTS AND DISCUSSION

ORF3-induced cellular detachment of human embryonic kidney 293T cells. Previous studies indicated that PCV2ORF3 is involved in apoptotic death of porcine and simian cells (14) and PCV2-associated pathology in pigs (9). Here, we hypothesized that if PCV2ORF3 is a major determinant for the virulence of PCV2, the analogous protein derived from the nonpathogenic PCV1 would not be able to kill cells. Upon transfection with an expression plasmid for eGFP-PCV1ORF3, human embryonic kidney 293T cells displayed morphological changes with a shrunken, grape-like appearance (Fig. 1A). Quantitative analysis of detached and adherent 293T cell numbers showed that cellular detachment was significantly higher in eGFP-PCV1ORF3-transfected cells compared to eGFP-PCV2ORF3- and eGFP-transfected cells ($P < 0.05$) (Fig. 1B). Etoposide, an apoptosis-inducing substance, likewise induced significant cellular detachment ($P < 0.05$). No significant difference in cellular detachment was observed between eGFP-PCV2ORF3- and eGFP-transfected cell populations. *PCVORF3* coding sequences cloned into a retroviral expression vector led to similar results (data not shown). Immunoblot analysis revealed that eGFP-PCV1ORF3 was predominantly seen in the detached, but not the adherent cell fraction (Fig.

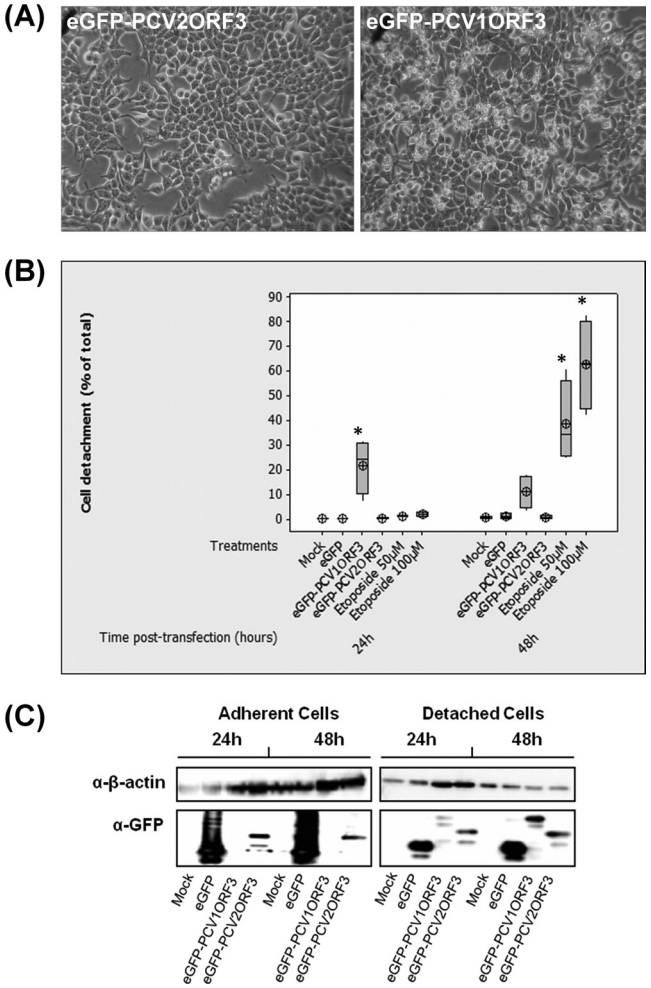

FIG. 1. Cell detachment in 293T cells. (A) Phase-contrast microscopy 24 h after transfection shows cells with shrunken, grape-like appearance in eGFP-PCV1ORF3-transfected cells and not in eGFP-PCV2ORF3-transfected cells. (B) Percentage of detached cells from four independent experiments ($n = 4$). Cellular detachment values that are significantly different ($P < 0.05$) from the values for negative controls, e.g., mock and eGFP, are indicated by an asterisk. The target symbol, the horizontal line in the box, and the box denote the mean, median, and interquartile range, respectively. (C) Separation of cells into adherent and detached cell fractions and the detection of eGFP-PCV1ORF3 predominantly in the detached cell fraction. Whole-cell extracts were resolved by 13% SDS-PAGE, transferred onto PVDF membranes, and detected by anti-GFP antibody (α-GFP). β-Actin was used as a protein loading control. α-β-actin, anti-β-actin antibody.

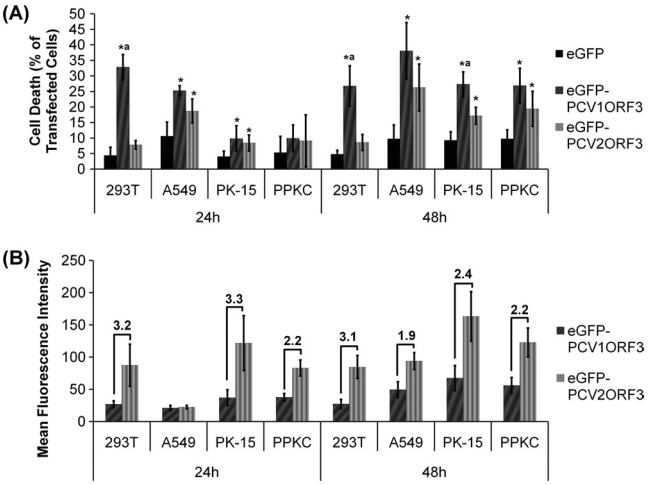

FIG. 2. Cell viability in various cell lines transfected with different ORF3 variants. Values are the means ± standard errors of the means (error bars represent 95% confidence interval for the mean) from at least three independent experiments ($n \geq 3$). (A) Percentage of cell death in transfected cells. Cell death values that are significantly different ($P < 0.05$) from the cell death values for eGFP-transfected cells (*) and eGFP-PCV2ORF3-transfected cells (a) are indicated above the bars. (B) Relative protein expression level on a per cell basis as measured by mean fluorescence intensity. The numbers above the bars indicate the average fold differences in mean fluorescence intensities.

1C). In summary, when expressed in 293T cells, PCV1ORF3 caused cellular detachment, while PCV2ORF3 did not. This result was unexpected, since PCV2ORF3 was previously reported to be cytotoxic in simian Cos-7 and porcine PK-15 cell lines (14); however, human cell types exposed to PCV2ORF3 as well as cytotoxicity of PCV1ORF3 had not been analyzed previously.

ORF3-induced cell death is cell type specific. As it was possible that dead cells could have remained adherent to the plate and that detached cells were not dead but had simply lost the ability to adhere, cytotoxicity leading to cell death was further assessed with PI staining. PI penetrates and stains only dead cells.

As shown in Fig. 2A, eGFP-PCV1ORF3 induced significantly more cell death ($P < 0.05$) than eGFP in all four cell lines tested. eGFP-PCV1ORF3 also induced significantly more cell death ($P < 0.05$) than eGFP-PCV2ORF3 did in both 293T and PK-15 cell lines despite a two- to threefold-lower level of eGFP-PCV1ORF3 protein expression compared to that of eGFP-PCV2ORF3 on a per cell basis, as measured by mean fluorescence intensity (Fig. 2B). Thus, the observed higher toxicity of eGFP-PCV1ORF3 was not the result of higher protein expression. eGFP-PCV2ORF3 induced significant cell death ($P < 0.05$) in A549, PK-15, and PPKC cells, but not in 293T cells. Neither eGFP-PCV1ORF3 nor eGFP-PCV2ORF3 induced significant cell death in bystander, nontransfected cells (data not shown), suggesting that an intrinsic death pathway was triggered by ORF3 leading to cell death. It has been suggested that ORF3s from different genogroups may confer differences in PCV2 virulence (31). Therefore, ORF3s from different genogroups were tested for differences in cytotoxicity, but significant difference in cell death was not observed between ORF3 from PCV2a and PCV2b genogroups (data not shown). Hence, two PCV2ORF3 sequences, which differ by 4 amino acids (aa), were presented interchangeably in this report.

Our results show that ORF3 proteins from PCV1 and PCV2 are capable of inducing cell death in a cell-specific manner, as variations in susceptibility to ORF3-induced cell death were observed between different cell types and within each cell type. In particular, human 293T cells were not as susceptible to eGFP-PCV2ORF3-induced cell death as other cell lines were. Within a population of one cell type, a large proportion of cells that expressed eGFP-PCV1ORF3 did not undergo cell death.

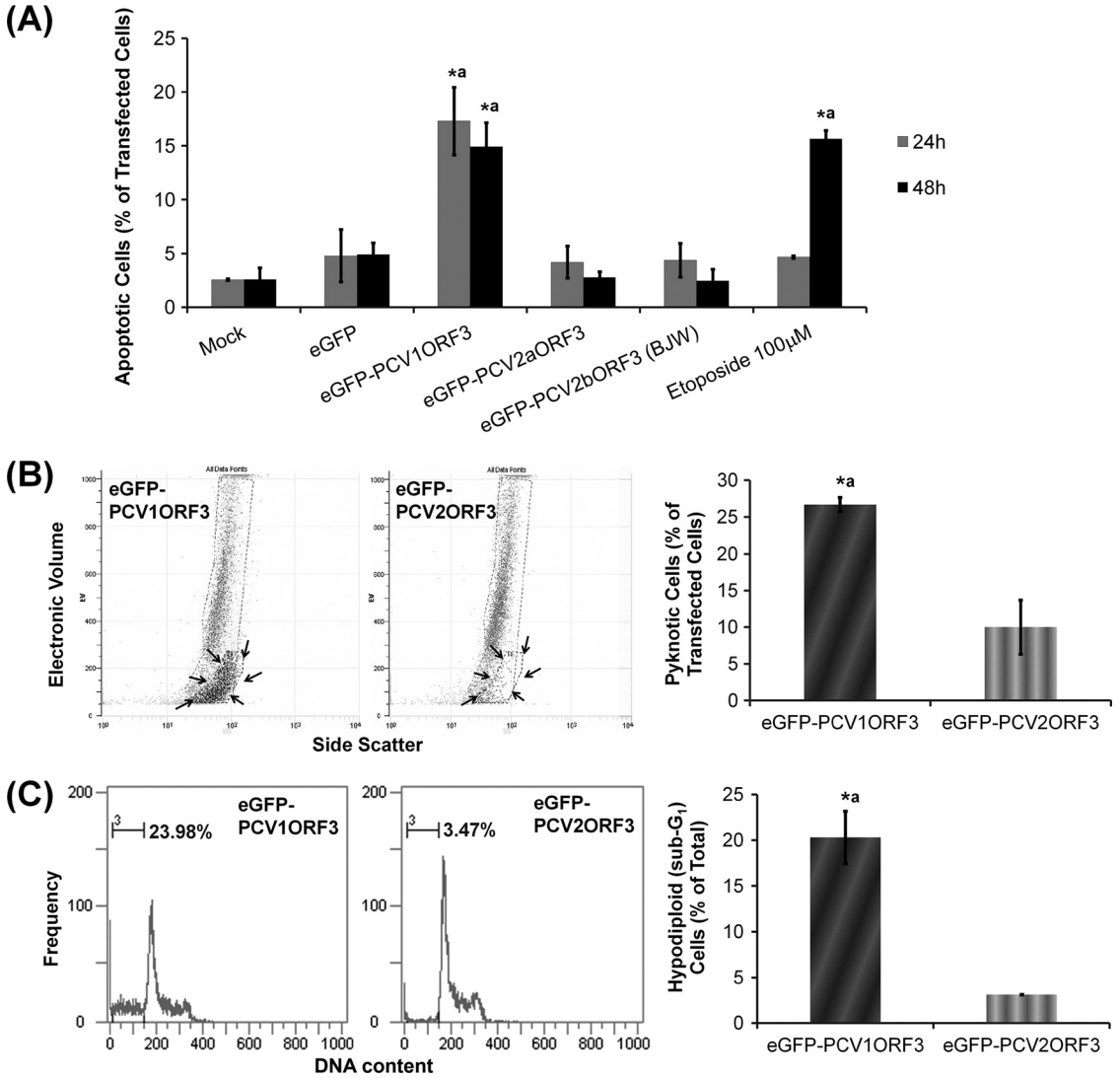

FIG. 3. Apoptosis assay results in 293T cells. Values that are significantly different ($P < 0.05$) from the values for negative controls, e.g., mock- or eGFP-transfected cells (*), and eGFP-PCV2ORF3-transfected cells (a) are indicated above the bars. Error bars represent 95% confidence interval for the standard error of the mean from at least two independent experiments ($n \geq 2$). (A) Percentage of PS externalization in transfected cells. (B) Percentage of pyknosis in transfected cells. The subpopulation of pyknotic cells is circled with a broken line and indicated by black arrows. (C) Percentage of cells with hypodiploid (apoptotic) DNA content.

Similarly, it has been reported that cells from different origins vary in their tolerance and responses to apoptosis-inducing agents, such as lithium chloride (15, 35). Therefore, it is possible that ORF3 is proapoptotic but that it is the state of the cellular host that determines the final outcome of virus-cell interactions.

PCV1ORF3 induces caspase-dependent apoptosis. To assess whether cell death induced by PCV1ORF3 occurred via apoptosis similar to what has been reported for PCV2ORF3 (14), PS externalization as an apoptotic marker was analyzed. During apoptosis, PS molecules become externalized to the outer surface of the cell membrane (18). This externalization is important for macrophage recognition, phagocytosis, and clearance of apoptotic cells without causing an inflammatory response (3, 19). In apoptotic cells, annexin V binds to these externalized PS molecules (1, 22, 28, 30) while PI or 7-AAD will not penetrate and stain these cells. Figure 3A shows that 293T cells transfected with eGFP-PCV1ORF3 had a significantly higher percentage of apoptotic cells (AV-PE positive, 7-AAD negative) than cells transfected with eGFP or eGFP-PCV2ORF3. Likewise, control cells treated with etoposide had a significantly higher percentage of apoptotic cells than mock-transfected cells did.

In addition to this biochemical marker, the traditional specific morphological aspects of apoptosis, such as rounding-up of cells (Fig. 1) and reduction of cellular volume or pyknosis (Fig. 3B), were also observed for eGFP-PCV1ORF3-transfected 293T cells. The subpopulation of cells with pyknosis, as demonstrated by lower electronic volume (EV) by FACS analysis, was found to be identical with the subpopulation of cells that were apoptotic (AV-PE positive, 7-AAD negative) (Fig. 4C). Cell cycle analysis (Fig. 3C), which showed the presence

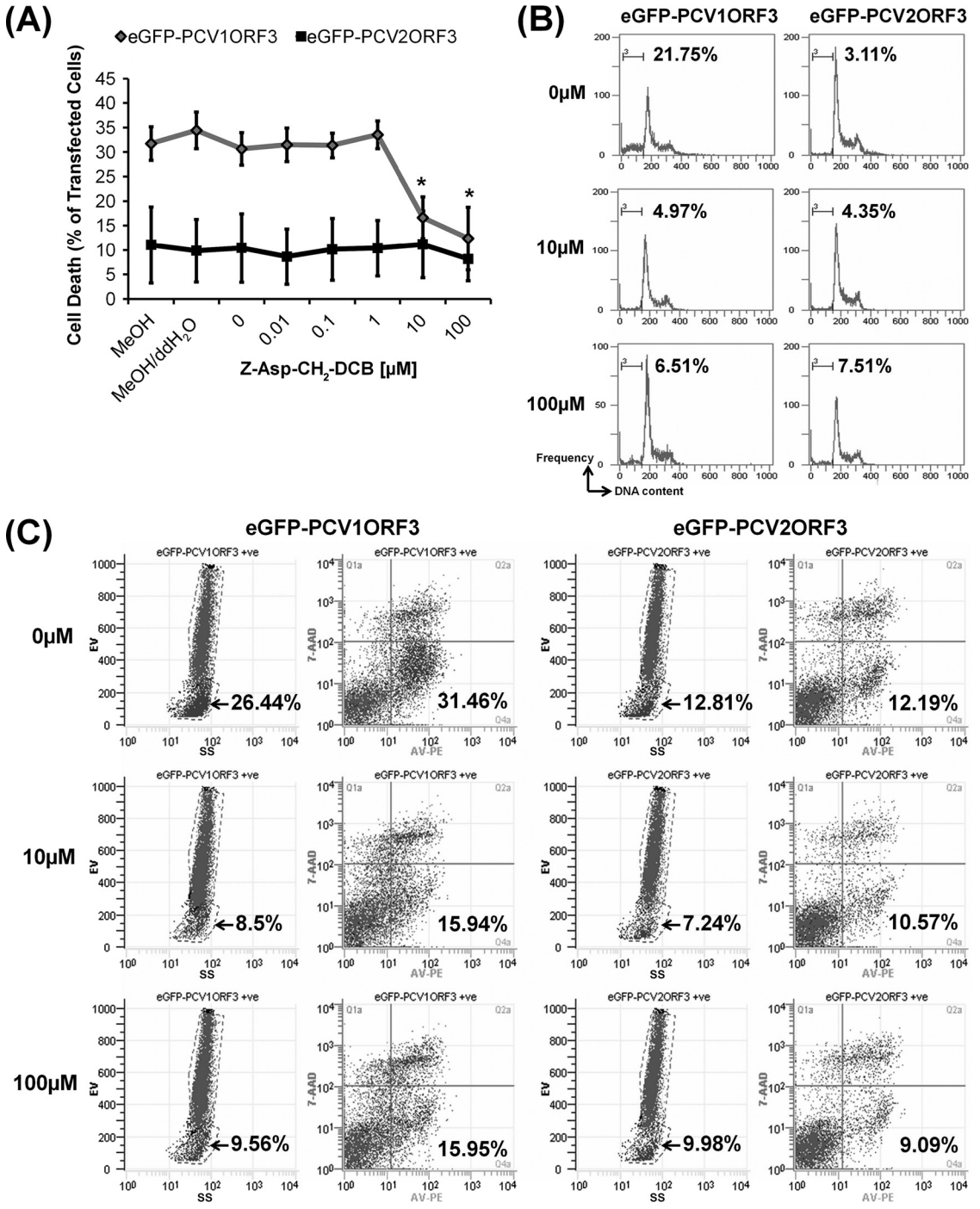

FIG. 4. Pancaspase inhibitor (Z-Asp-CH_2-DCB) assays in 293T cells at 24 h posttransfection. (A) Effects of various concentrations of Z-Asp-CH_2-DCB on the percentage of cell death induced by eGFP-PCV1ORF3. Error bars represent 95% confidence interval for the standard error of the mean from three independent experiments ($n = 3$). Values that are significantly different ($P < 0.05$) are indicated by an asterisk. MeOH, methanol; ddH_2O, double-distilled water. (B) Effects of various concentrations of Z-Asp-CH_2-DCB (0, 10, and 100 μM) on the percentage of cells with hypodiploid DNA content. (C) Effects of various concentrations of Z-Asp-CH_2-DCB (0, 10, and 100 μM) on eGFP-PCV1ORF3-induced pyknosis (leftmost columns for both eGFP-PCV1ORF3 and eGFP-PCV2ORF3) and eGFP-PCV1ORF3-induced PS externalization (rightmost columns for both eGFP-PCV1ORF3 and eGFP-PCV2ORF3). For eGFP-PCV1ORF3-induced pyknosis (the leftmost columns for both eGFP-PCV1ORF3 and eGFP-PCV2ORF3), electronic volume (EV) is shown on the *y* axis, and side scatter (SS) is shown on the *x* axis. The arrow indicates the percentage of pyknosis in transfected cells. For eGFP-PCV1ORF3-induced PS externalization (rightmost columns for both eGFP-PCV1ORF3 and eGFP-PCV2ORF3), 7-AAD is shown on the *y* axis, and AV-PE is shown on the *x* axis. The bottom right quadrant shows the percentage of PS externalization in transfected cells. +ve, positive.

of hypodiploid (sub-G_1) cells with lower DNA content in eGFP-PCV1ORF3-transfected population, further confirmed the apoptotic capability of PCV1ORF3. eGFP-PCV1ORF3-induced apoptotic cell death was inhibitable by Z-Asp-CH_2-DCB, as increasing concentrations (10 μM and 100 μM) of this broad-spectrum caspase inhibitor significantly reduced the percentage of eGFP-PCV1ORF3-mediated apoptotic cell death ($P < 0.05$) (Fig. 4A) by diminishing the subpopulation of cells with hypodiploid DNA content (Fig. 4B), pyknosis, and PS externalization (Fig. 4C). Caution was taken when using the term caspase dependent, because although Z-Asp-CH_2-DCB is supposed to specifically inhibit caspases, a family of cysteine proteases, it has been shown that another broad-spectrum caspase inhibitor, Z-VAD-FMK (benzyloxycarbonyl-Val-Ala-DL-Asp conjugated to fluoromethylketone), can also inhibit calpains and cathepsins (24), especially at high concentration (>10 μM), and can associate with targets that are not part of a caspase-dependent pathway by binding to other cysteine proteases and proteins (12). Since only a 10 μM concentration of the pancaspase inhibitor was used to inhibit PCV1ORF3-mediated apoptotic cell death, it should be safe to assume that PCV1ORF3-mediated apoptotic cell death is caspase dependent. Future experiments using small interfering RNA (siRNA) to knock down different caspases will confirm the involvement of specific caspases.

These results demonstrate that PCV1ORF3 induced apoptotic cell death via a caspase-dependent pathway, with PCV1ORF3 being a more potent inducer of cell death than PCV2ORF3. Yet, only PCV2, not PCV1, leads to lymphocyte depletion and disease in pigs. Similarly, PCV1 persistently infects PK-15 cells without any obvious cytopathic effects (7, 32, 33), whereas PCV2 infection appears to kill PK-15 cells. As ORF3 protein expression has not been reported over the course of PCV1 infection, either *in vitro* or *in vivo*, it is possible that the expression of PCV1ORF3 is tightly regulated or even not occurring *in vitro* and conceivably *in vivo* as well. Perhaps the lack of ORF3 expression in PCV1 infection in pigs incapacitates the virus from causing PCVAD. Alternatively, if PCV1ORF3 were expressed *in vivo*, the ability to induce apoptosis to a greater extent could render PCV1 nonpathogenic, because PCV1-infected cells would be recognized, phagocytosed, and cleared by the immune cells without an activation of inflammatory responses.

PCV1ORF3 induces PARP cleavage. Activated caspases are capable of cleaving and thereby inactivating PARP molecules, a DNA repair enzyme, leading to apoptosis (2, 20, 27, 29). To further elucidate the mechanism of apoptosis induced by PCV1ORF3, we analyzed PARP cleavage. As expected, eGFP-PCV2ORF3 did not induce PARP cleavage (Fig. 5A), because it did not cause significant apoptotic cell death in 293T cells (Fig. 1 to 3). This was further confirmed when a pancaspase inhibitor did not influence the level of PARP cleavage in eGFP-PCV2ORF3-transfected cells (Fig. 5B). However, immunoblot analysis (Fig. 5A) showed a strong signal for the cleaved 27-kDa PARP fragment in eGFP-PCV1ORF3-transfected cells and in control cells treated with etoposide. Interestingly, eGFP-PCV1ORF3-mediated PARP cleavage was not reduced in the presence of 10 μM Z-Asp-CH_2-DCB but was reduced in the presence of a higher concentration (100 μM) of this pancaspase inhibitor (Fig. 5B). As indicated previously, it

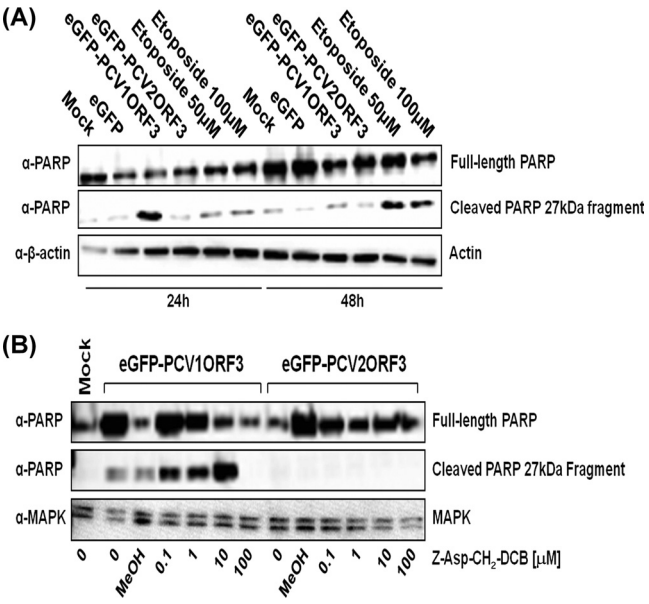

FIG. 5. PARP cleavage assay in 293T cells. (A) Detection of the cleaved 27-kDa PARP fragment in etoposide-treated and eGFP-PCV1ORF3-transfected cells. (B) Effects of various micromolar concentrations of Z-Asp-CH_2-DCB on eGFP-PCV1ORF3-mediated PARP cleavage at 24 h posttransfection. Whole-cell extracts were resolved by 13% SDS-PAGE, transferred onto PVDF membranes, and detected by anti-PARP antibody (α-PARP). Either β-actin or MAPK was used as a protein loading control.

is possible that the pancaspase inhibitor can be caspase nonspecific when used at a high concentration (12, 24). PARP cleavage may occur independently of cell death, and multiple pathways might be activated by PCV1ORF3. Transforming growth factor β1, a cytokine that plays a role in many physiological processes, such as cell proliferation, differentiation, apoptosis, and growth inhibition, has also been shown to induce caspase-dependent apoptosis and caspase-independent PARP cleavage (34), similar to the data on PCV1ORF3 presented here. Taken together, these results show that PCV1ORF3 activates PARP cleavage that might be dissociated from a caspase-dependent apoptotic cell death pathway.

Effects of modified PCVORF3 proteins. Comparison of *PCV1* and *PCV2 ORF*3 sequences revealed a consistent single-nucleotide substitution resulting in a PCV2ORF3 protein that is truncated compared to PCV1ORF3. The stop codon is conserved in most published PCV2 genomes, making it likely that it preserves virus survival of PCV2 in pigs. The truncated PCV2ORF3 could either be associated with an unknown gain of function or with an attenuation of an otherwise even more detrimental PCV2 virus, i.e., a PCV2 with an elongated ORF3. To test the latter hypothesis, we generated truncated PCV1ORF3 (eGFP-PCV1ORF3:Y105*) and elongated PCV2ORF3 (eGFP-PCV2ORF3:*105Y). Figure 6A illustrates that eGFP-PCV1ORF3:Y105* induced significantly less cell death than eGFP-PCV1ORF3 did, despite two- to ninefold-higher levels of expression (Fig. 6C). eGFP-PCV2ORF3:*105Y induced the same level of cell death as eGFP-PCV2ORF3 did (Fig. 6B), despite two- to fivefold-lower levels of expression (Fig. 6D). The finding that the elongated ORF3

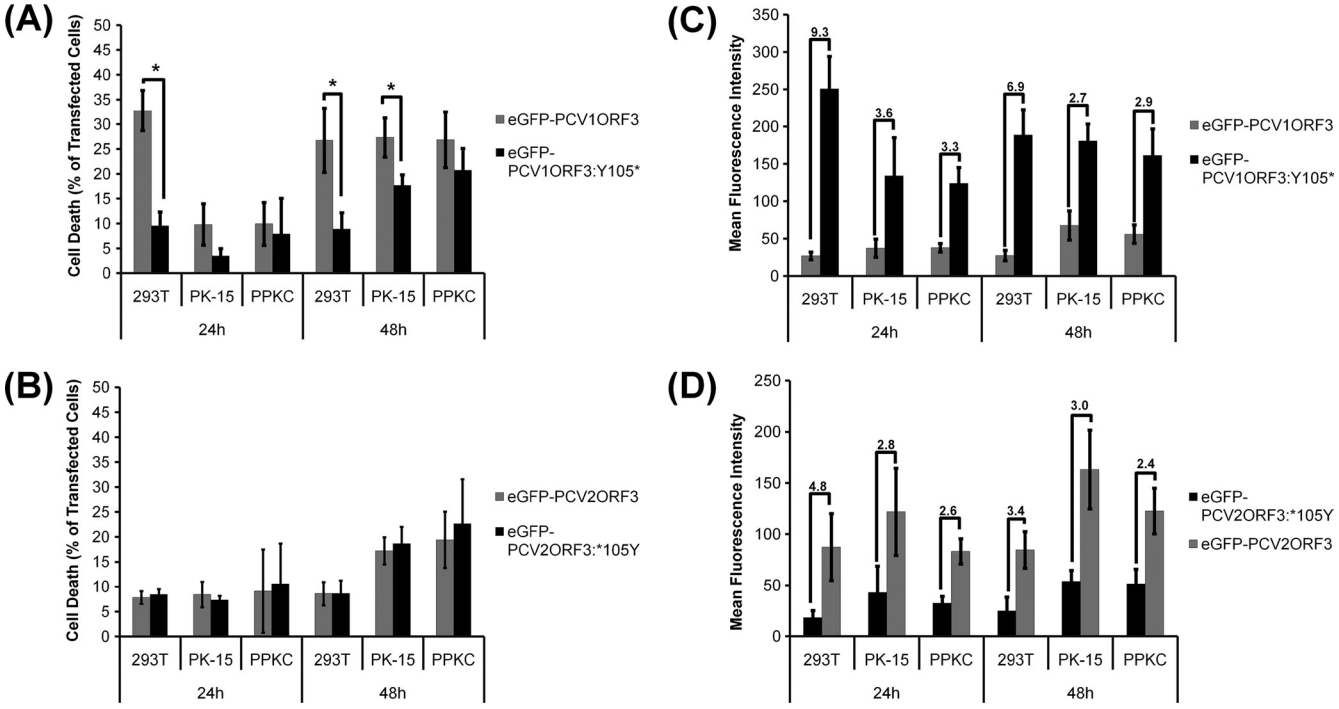

FIG. 6. Cytotoxicity of mutated PCVORF3 proteins. Error bars represent 95% confidence interval for the standard error of the mean from at least three independent experiments ($n \geq 3$). (A and B) Percentage of cell death in transfected cells. Cell death values that are significantly different ($P < 0.05$) are indicated by brackets and an asterisk. (C and D) Relative protein expression level on a per cell basis as measured by mean fluorescence intensity. The numbers above the bars indicate the average fold differences in mean fluorescence intensities.

of PCV2 failed to induce an increased level of cell death may be attributed to the second stop codon at amino acid position 169 downstream of the first stop codon at amino acid position 105, making this elongated PCV2ORF3 38 aa shorter than that of the authentic PCV1ORF3. The second stop codon (aa169), however, is not consistently found among the strains of PCV2 and appears to be random. Those PCV2 strains without the stop codon at aa169 lacked another stop codon downstream, e.g., at aa206 as in PCV1ORF3. The effect of removal of the second stop codon at aa169 was not investigated further, because this stop codon is not consistently found in nature among PCV2 strains. Overall, the ability to induce cell death by both modified ORF3 constructs resembles that of PCV2ORF3. This suggests that the first 104 aa contain a conserved domain capable of inducing cell death, whereas the C terminus of PCV1ORF3 contains a domain possibly responsible for enhancing cell death.

In summary, our findings reveal that PCV1ORF3 is a potent inducer of apoptotic cell death and is more cytotoxic than PCV2ORF3 is under the given experimental conditions. The fact that PCV1 does not appear to be cytopathogenic for cultured cells or for infected pigs could suggest that this protein is not expressed in the course of infection or that other virus or host proteins counteract its action, thus rendering the virus nonpathogenic. Alternatively, during the course of PCV1 infection, PCV1ORF3 may be expressed only in those cells that are refractive to PCV1ORF3-mediated apoptosis. The latter hypothesis is supported by our results demonstrating that different cell types exhibited various levels of susceptibility to ORF3-induced cell death. The ability to induce apoptosis to a greater extent in infected cells may actually be more detrimental to the virus, as it allows the immune cells to recognize and clear infected cells without inducing inflammatory responses.

Similar to PCV1ORF3, expression of PCV2ORF3 in pigs that were naturally infected with PCV2 has not been verified. For an ORF3 protein to be the molecular pathogenic factor for PCVAD, the presence of ORF3 antigens or antibodies against ORF3 should be consistently or at least demonstrated in pigs that are naturally infected with PCV2 or diagnosed with PCVAD. A recent report has shown that ORF3 is dispensable for PCV2 replication and the lack of its expression has little, if any, impact on PCV2 pathogenicity (8). It is also debatable whether apoptosis is the mechanism of PCV2-mediated immunosuppression because several studies supported the role of apoptosis (10, 26), but others did not (11, 16, 23). ORF3 and, particularly, ORF3-mediated apoptosis may not be a major or the sole determinant of PCV2 pathogenicity. Interestingly, however, when pigs were experimentally infected with a mutant PCV2 with a nonfunctional *ORF3* gene, they mounted a normal immune response, were capable of clearing viral infection, and exhibited little if any pathology (9). In addition, recent findings indicate that DNA immunization with plasmid-derived PCV2ORF3 in mice (25) and experimental infection of pigs with wild-type PCV2 appeared to reduce the animal's ability to mount an immune response against PCV2 and to clear virus infection (9). It is possible that PCV2ORF3 may be involved in immunosuppression but not via its apoptotic capability.

ACKNOWLEDGMENTS

We thank Avril Hatherell, Sampson Law, Sandi Nishikawa, G. van Marle, F. Jirik, and R. Yates and the DNA and Flow Cytometry Core Facilities at the University of Calgary for training and technical support.

This work was supported by the Natural Sciences and Engineering Research Council (NSERC), Alberta Agriculture Consortium, and University of Calgary Faculties of Medicine and Veterinary Medicine.

REFERENCES

1. **Andree, H. A., C. P. Reutelingsperger, R. Hauptmann, H. C. Hemker, W. T. Hermens, and G. M. Willems.** 1990. Binding of vascular anticoagulant alpha (VAC alpha) to planar phospholipid bilayers. J. Biol. Chem. **265:**4923–4928.
2. **Boulares, A. H., A. G. Yakovlev, V. Ivanova, B. A. Stoica, G. Wang, S. Iyer, and M. Smulson.** 1999. Role of poly(ADP-ribose) polymerase (PARP) cleavage in apoptosis. Caspase 3-resistant PARP mutant increases rates of apoptosis in transfected cells. J. Biol. Chem. **274:**22932–22940.
3. **Duvall, E., A. H. Wyllie, and R. G. Morris.** 1985. Macrophage recognition of cells undergoing programmed cell death (apoptosis). Immunology **56:**351–358.
4. **Ellis, J., L. Hassard, E. Clark, J. Harding, G. Allan, P. Willson, J. Strokappe, K. Martin, F. McNeilly, B. Meehan, D. Todd, and D. Haines.** 1998. Isolation of circovirus from lesions of pigs with postweaning multisystemic wasting syndrome. Can. Vet. J. **39:**44–51.
5. **Finsterbusch, T., and A. Mankertz.** 2009. Porcine circoviruses–small but powerful. Virus Res. **143:**177–183.
6. **Harding, J. C., C. D. Baker, A. Tumber, K. A. McIntosh, S. E. Parker, D. M. Middleton, J. E. Hill, J. A. Ellis, and S. Krakowka.** 2008. Porcine circovirus-2 DNA concentration distinguishes wasting from nonwasting pigs and is correlated with lesion distribution, severity, and nucleocapsid staining intensity. J. Vet. Diagn. Invest. **20:**274–282.
7. **Hattermann, K., C. Roedner, C. Schmitt, T. Finsterbusch, T. Steinfeldt, and A. Mankertz.** 2004. Infection studies on human cell lines with porcine circovirus type 1 and porcine circovirus type 2. Xenotransplantation **11:**284–294.
8. **Juhan, N. M., T. LeRoith, T. Opriessnig, and X. J. Meng.** 2010. The open reading frame 3 (ORF3) of porcine circovirus type 2 (PCV2) is dispensable for virus infection but evidence of reduced pathogenicity is limited in pigs infected by an ORF3-null PCV2 mutant. Virus Res. **147:**60–66.
9. **Karuppannan, A. K., M. H. Jong, S. H. Lee, Y. Zhu, M. Selvaraj, J. Lau, Q. Jia, and J. Kwang.** 2009. Attenuation of porcine circovirus 2 in SPF piglets by abrogation of ORF3 function. Virology **383:**338–347.
10. **Kiupel, M., G. W. Stevenson, E. J. Galbreath, A. North, H. HogenEsch, and S. K. Mittal.** 2005. Porcine circovirus type 2 (PCV2) causes apoptosis in experimentally inoculated BALB/c mice. BMC Vet. Res. **1:**7.
11. **Krakowka, S., J. Ellis, F. McNeilly, B. Meehan, M. Oglesbee, S. Alldinger, and G. Allan.** 2004. Features of cell degeneration and death in hepatic failure and systemic lymphoid depletion characteristic of porcine circovirus-2-associated postweaning multisystemic wasting disease. Vet. Pathol. **41:**471–481.
12. **Kroemer, G., L. Galluzzi, P. Vandenabeele, J. Abrams, E. S. Alnemri, E. H. Baehrecke, M. V. Blagosklonny, W. S. El-Deiry, P. Golstein, D. R. Green, M. Hengartner, R. A. Knight, S. Kumar, S. A. Lipton, W. Malorni, G. Nuñez, M. E. Peter, J. Tschopp, J. Yuan, M. Piacentini, B. Zhivotovsky, and G. Melino.** 2009. Classification of cell death: recommendations of the Nomenclature Committee on Cell Death 2009. Cell Death Differ. **16:**3–11.
13. **Liu, J., I. Chen, Q. Du, H. Chua, and J. Kwang.** 2006. The ORF3 protein of porcine circovirus type 2 is involved in viral pathogenesis in vivo. J. Virol. **80:**5065–5073.
14. **Liu, J., I. Chen, and J. Kwang.** 2005. Characterization of a previously unidentified viral protein in porcine circovirus type 2-infected cells and its role in virus-induced apoptosis. J. Virol. **79:**8262–8274.
15. **Lucas, K. C., D. A. Hart, and R. W. Becker.** 2010. Porcine proximal tubular cells (LLC-PK1) are able to tolerate high levels of lithium chloride in vitro: assessment of the influence of 1–20 mM LiCl on cell death and alterations in cell biology and biochemistry. Cell Biol. Int. **34:**225–233.
16. **Mandrioli, L., G. Sarli, S. Panarese, S. Baldoni, and P. S. Marcato.** 2004. Apoptosis and proliferative activity in lymph node reaction in postweaning multisystemic wasting syndrome (PMWS). Vet. Immunol. Immunopathol. **97:**25–37.
17. **Mankertz, A., J. Mankertz, K. Wolf, and H. J. Buhk.** 1998. Identification of a protein essential for replication of porcine circovirus. J. Gen. Virol. **79:**381–384.
18. **Martin, S. J., C. P. Reutelingsperger, A. J. McGahon, J. A. Rader, R. C. van Schie, D. M. LaFace, and D. R. Green.** 1995. Early redistribution of plasma membrane phosphatidylserine is a general feature of apoptosis regardless of the initiating stimulus: inhibition by overexpression of Bcl-2 and Abl. J. Exp. Med. **182:**1545–1556.
19. **Morris, R. G., A. D. Hargreaves, E. Duvall, and A. H. Wyllie.** 1984. Hormone-induced cell death. 2. Surface changes in thymocytes undergoing apoptosis. Am. J. Pathol. **115:**426–436.
20. **Nicholson, D. W., A. Ali, N. A. Thornberry, J. P. Vaillancourt, C. K. Ding, M. Gallant, Y. Gareau, P. R. Griffin, M. Labelle, Y. A. Lazebnik, N. A. Munday, S. M. Raju, M. E. Smulson, T.-T. Yamin, V. L. Yu, and D. K. Miller.** 1995. Identification and inhibition of the ICE/CED-3 protease necessary for mammalian apoptosis. Nature **376:**37–43.
21. **Opriessnig, T., X. J. Meng, and P. G. Halbur.** 2007. Porcine circovirus type 2 associated disease: update on current terminology, clinical manifestations, pathogenesis, diagnosis, and intervention strategies. J. Vet. Diagn. Invest. **19:**591–615.
22. **Raynal, P., and H. B. Pollard.** 1994. Annexins: the problem of assessing the biological role for a gene family of multifunctional calcium- and phospholipid-binding proteins. Biochim. Biophys. Acta **1197:**63–93.
23. **Resendes, A. R., N. Majó, J. Segalés, E. Mateu, M. Calsamiglia, and M. Domingo.** 2004. Apoptosis in lymphoid organs of pigs naturally infected by porcine circovirus type 2. J. Gen. Virol. **85:**2837–2844.
24. **Schotte, P., W. Declercq, S. Van Huffel, P. Vandenabeele, and R. Beyaert.** 1999. Non-specific effects of methyl ketone peptide inhibitors of caspases. FEBS Lett. **442:**117–121.
25. **Shen, H. G., J. Y. Zhou, X. Zhang, Z. Y. Huang, J. L. He, and Y. Yan.** 2009. Interference of porcine circovirus type 2 ORF2 immunogenicity by ORF1 and ORF3 mixed DNA immunizations in mice. Virology **393:**104–111.
26. **Shibahara, T., K. Sato, Y. Ishikawa, and K. Kadota.** 2000. Porcine circovirus induces B lymphocyte depletion in pigs with wasting disease syndrome. J. Vet. Med. Sci. **62:**1125–1131.
27. **Simbulan-Rosenthal, C. M., D. S. Rosenthal, S. Iyer, H. Boulares, and M. E. Smulson.** 1999. Involvement of PARP and poly(ADP-ribosyl)ation in the early stages of apoptosis and DNA replication. Mol. Cell. Biochem. **193:**137–148.
28. **Tait, J. F., D. Gibson, and K. Fujikawa.** 1989. Phospholipid binding properties of human placental anticoagulant protein-I, a member of the lipocortin family. J. Biol. Chem. **264:**7944–7949.
29. **Tewari, M., L. T. Quan, K. O'Rourke, S. Desnoyers, Z. Zeng, D. R. Beidler, G. G. Poirier, G. S. Salvesen, and V. M. Dixit.** 1995. Yama/CPP32 beta, a mammalian homolog of CED-3, is a CrmA-inhibitable protease that cleaves the death substrate poly(ADP-ribose) polymerase. Cell **81:**801–809.
30. **Thiagarajan, P., and J. F. Tait.** 1990. Binding of annexin V/placental anticoagulant protein I to platelets. Evidence for phosphatidylserine exposure in the procoagulant response of activated platelets. J. Biol. Chem. **265:**17420–17423.
31. **Timmusk, S., P. Wallgren, I. M. Brunborg, F. H. Wikström, G. Allan, B. Meehan, M. McMenamy, F. McNeilly, L. Fuxler, K. Belák, D. Põdersoo, T. Saar, M. Berg, and C. Fossum.** 2008. Phylogenetic analysis of porcine circovirus type 2 (PCV2) pre- and post-epizootic postweaning multisystemic wasting syndrome (PMWS). Virus Genes **36:**509–520.
32. **Tischer, I., H. Gelderblom, W. Vettermann, and M. A. Koch.** 1982. A very small porcine virus with circular single-stranded DNA. Nature **295:**64–66.
33. **Tischer, I., R. Rasch, and G. Tochtermann.** 1974. Characterization of papovavirus-and picornavirus-like particles in permanent pig kidney cell lines. Zentralbl. Bakteriol. Orig. A **226:**153–167.
34. **Yang, Y., S. Zhao, and J. Song.** 2004. Caspase-dependent apoptosis and -independent poly(ADP-ribose) polymerase cleavage induced by transforming growth factor beta1. Int. J. Biochem. Cell Biol. **36:**223–234.
35. **Zhang, W. V., M. Jüllig, A. R. Connolly, and N. S. Stott.** 2005. Early gene response in lithium chloride induced apoptosis. Apoptosis **10:**75–90.